Plasma-Modified SnO2 Nanowires for Enhanced Gas Sensing

ARTICLE *in* THE JOURNAL OF PHYSICAL CHEMISTRY C · APRIL 2010

Impact Factor: 4.77 · DOI: 10.1021/jp101072f

Plasma-Modified SnO_2 Nanowires for Enhanced Gas Sensing

Jun Pan,[†] Rajesh Ganesan,[‡] Hao Shen,[†] and Sanjay Mathur*[,†,‡]

Institute of Inorganic and Materials Chemistry, University of Cologne, Cologne, D-50939 Germany, and Leibniz Institute of New Materials, Saarbruecken, D-66123 Germany

Received: February 4, 2010; Revised Manuscript Received: March 18, 2010

Tin oxide (SnO_2) nanowires grown by chemical vapor deposition were modified by Ar/O_2 plasma treatment through preferential etching of the lattice oxygen atoms, which produced nonstoichiometric surface compositions that imparted a manyfold higher sensitivity toward gas absorption on such surfaces. Microstructures of as-grown and plasma-treated SnO_2 nanowires confirmed the gradual change in the chemical composition and morphologies. Surficial disorder caused by the bombardment of argon and oxygen ions present in the plasma was visible as a disordered overlayer in high-resolution TEM micrographs, when compared to single crystalline as-grown SnO_2 nanowires. Gas-sensing experiments on modified SnO_2 nanostructures showed higher sensitivity for ethanol gas at lower operating temperatures and exhibited an improved transduction response toward changing gas atmospheres, attributed to the increased concentration of oxygen vacancies on the surface of SnO_2 nanowires. Modulation of surface chemistry was also supported by photoluminescence and X-ray photoemission spectroscopy studies.

1. Introduction

One dimensional (1D) semiconductor nanostructures have stimulated considerable interest for scientific research because of their novel optical, electrical, magnetic, and mechanical properties owing to their unique structural dimensionality and possible quantum confinement effects.[1−6] The recent contribution to this field is the utilization of one-dimensional nanostructures (e.g, nanotubes, nanowires, and nanorods) as novel gas-sensing materials. The confinement effects in nanostructures are anticipated to enhance the three "S" features (sensitivity, selectivity, and stability) important for sensor technology. In addition, the proven higher sensitivity and lower operation temperature of gas sensors based on various nanostructured materials in diversified applications to detect and monitor traces of toxic and explosive gases in automobile and aerospace industries, food manufacturing concerns, medical, domestic, and security sectors have emerged.[2] The enhanced ability of nanostructures to detect even tiny gas concentrations is due to their high surface-to-volume ratio, which augments the influence of surface states and thus transduction phenomemon.[7−13]

As an intrinsic n-type semiconductor, SnO_2 has been extensively exploited in applications related to gas sensing. Tin oxide nanowires are excellent transducer elements because of the large surface sensing area and the 1D carrier transport mechanism.[5] This offers novel and unique potential to modulate the gas-sensing efficiency by making the whole nanowire as a conduction channel being able to respond to the charge-transfer reaction occurring on the nanowire surface.[5,14,15] Numerous methods have been employed to synthesize tin oxide nanostructures, such as high-temperature vapor transport,[16] laser ablation of metallic Sn targets in an oxygen-containing atmosphere,[17] and thermal evaporation of high-purity metal oxide powder.[18] Among the above synthetic approaches for nanowire synthesis, decomposition of single molecular precursors on metal catalysts allows synthesizing different nanostructures with precisely defined chemical compositions, sizes, morphologies, and surface states. We have recently reported a molecule-based CVD process for growing tin oxide nanowires by catalyst-assisted decomposition of the molecular precursor, $Sn(O^tBu)_4$, which contains preformed Sn−O units,[7,8,15] also inherent to the solid-state SnO_2 material. The clear conversion of precursor into oxide material under elimination of molecular byproducts has been reported elsewhere.[19−21]

Stoichiometric tin oxide nanowires do not comply with the chemiresistor prerequisites evident in their marginal transducing property and high operation temperatures required for gas detection.[22] These inherent limitations can be overcome by doping the pure base material with metals and/or metal oxides, which leads to tunable physical and chemical properties, for instance, by creating Schottky barriers at metal−semiconductor interfaces and modulating the crystal fields near the interfaces.[23,24] We recently discovered that post growth modification of tin oxide films in capacitively coupled rf plasma leads to partial reduction of Sn(IV) species, creating a valence dynamics (Sn^{2+}, Sn^{3+}, and Sn^{4+}) on the surface, which substantially enhances their ethanol-sensing properties.[7] The partial reduction of SnO_2 deposits by the preferential etching of bridging oxygen species in the lattice eventually increases the sensor performance by its higher sensitivity with lower response and recovery times, which is accompanied by the reduction in operating temperature. Plasma-assisted modification of nanowires changes homogeneously the surface chemical composition without losing the single-crystalline nature and the characteristic high aspect ratio of nanowires. We, therefore, believe that, by controlling the gas species and power for plasma treatment, we can enhance the sensitivity of the tin oxide nanowire-based gas sensor. In addition, the surface etching is stable over several cycles and indicates that electronic factions from an equilibrium state driven by redox reactions. To date, many studies have focused on plasma-treated tin oxide film[25,26] and nanorods.[27,28] However, to our knowledge, little is known on the plasma-treatment of SnO_2 nanowires. More importantly, plasma treatment has been used to fabricate one-dimensional nanostructures or as a surface

* To whom correspondence should be addressed. Tel: +49-221-470-4107. Fax: +49-221-470-4899. E-mail: sanjay.mathur@uni-koeln.de.
[†] University of Cologne.
[‡] Leibniz Institute of New Materials.

10.1021/jp101072f
Published on Web 04/12/2010

TABLE 1: Description of the TTO Series of Tin Oxide NW Samples

samples	applied plasma power (W)	duration (s)
TO		
TTO 1	10	240
TTO 2	20	240
TTO 3	30	240
TTO 4	40	240
TTO 5	80	240

modification method; the mechanistic aspects of plasma treatment and their correlation to the enhanced gas-sensing performance have not been reported.

Herein, we investigate the adsorption of oxygen species (O^-, O_2^-, O_2^{2-}, etc.) on as-grown and plasma-modified SnO_2 single-crystalline nanowires and elaborate on the influence of surface chemistry and composition on the charge transduction induced by adsorption of gaseous analysis.

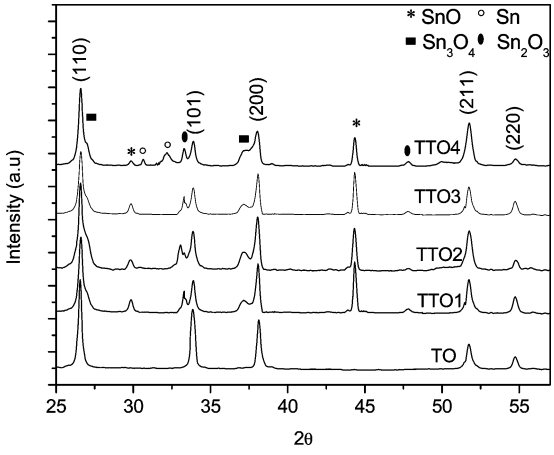

Figure 1. XRD patterns of as-deposited (TO) and plasma-treated (TTO) SnO_2 nanowires.

2. Experimental Section

Tin oxide nanowires were obtained through chemical vapor deposition of the molecular precursor, $Sn(O^tBu)_4$, which acts as a single delivery source for the elements Sn and O.[7] No additional oxygen source was required. The as-grown nanowires were exposed to rf plasma (Ar/O_2, 1:1) for 4 min at different power conditions to prepare TTO samples, which are denoted in the following text as TTO1 (10 W), TTO2 (20 W), TTO3 (30 W), TTO4 (40 W), and TTO5 (80 W), respectively (Table 1). Argon and oxygen with a flow rate of 10 and 15 sccm, respectively, were introduced in the PECVD system through mass flow controllers.

Room-temperature X-ray diffraction was performed with a Siemens D-500 diffractometer using CuKα radiation to record structural information and changes in pre- and post plasma-treated samples. Transmission electron microscopy (TEM) was performed with a TEM Philips 200 FEG (200 kV). Nanowire-based gas sensors were fabricated by contacting nanowire samples (as-prepared and plasma-treated) with gold wires and gold paste. Gas-sensing experiments were performed using a self-built PC-automated gas-sensing characterization system. Samples were mounted in the system with a chamber volume of 30 cm^3. Ethanol with a concentration of 100 ppm was mixed with synthetic air (flow rate = 15 sccm) and passed into the chamber maintained at accurate pressure using mass flow controllers. During the on/off gas-sensing measurement, the sensors were exposed (1 min) to the gas (on) and refreshed for 9 min by flushing dry air (off) at different operating temperatures (220−250 °C). The photoluminescence has been performed on an optical spectrometer operated on a 240 nm laser beam.

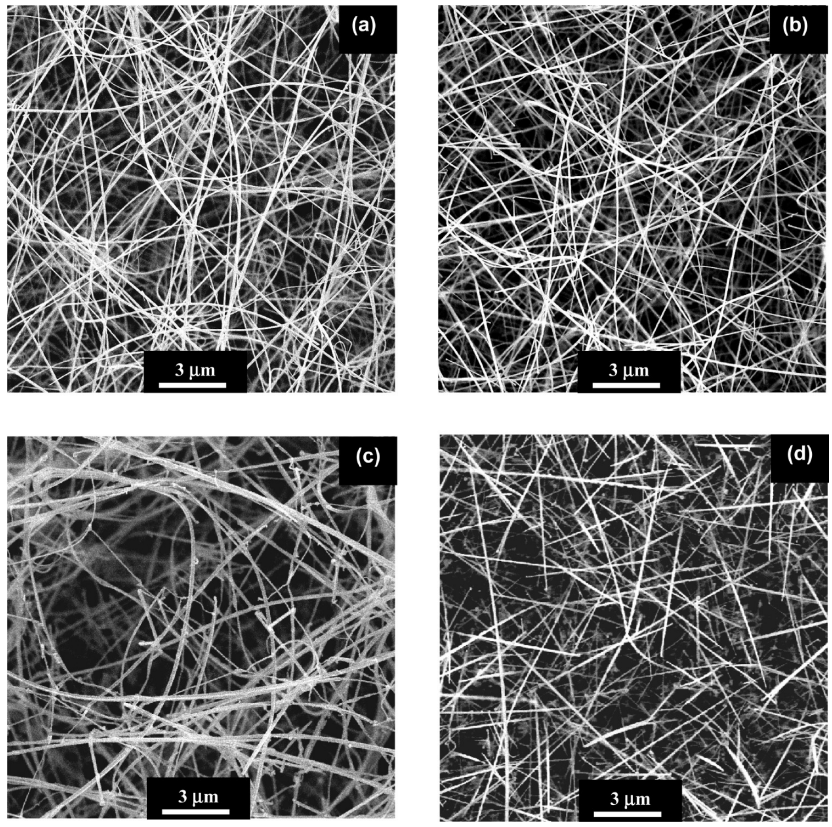

Figure 2. SEM micrographs of (a) as-deposited (TO) and plasma-treated (TTO) SnO_2 nanowire samples at (b) 10, (c) 40, and (d) 80 W.

3. Results and Discussion

Tin oxide nanowires grew following the well-known catalyst-assisted VLS growth mode.[7] X-ray diffraction patterns (Figure 1) of as-deposited and plasma-treated nanowire samples confirmed the nanowires to be constituted of tetragonal SnO_2 phase. The absence of any other phases confirmed the structural and chemical homogeneity of the as-deposited nanowires. The diffractograms of tin oxide nanowires exposed to plasma treatment at 10, 20, and 40 W showed incipient evolution of SnO, Sn_2O_3, and Sn_3O_4 as additional phases resulting apparently from gradual reduction of tetragonal SnO_2 due to removal of bridging oxygen atoms from the stoichiometric SnO_2. SnO_2 nanowires treated at 10, 20, 30, and 40 W showed a reduction in the peak intensity of the (110) reflection due to the creation of an amorphous overlayer on the SnO_2 crystalline core. The further increase in the plasma power up to 40 W (TTO4) generated more energetic ions and neutrals in plasma, which led to the formation of metallic Sn on the nanowire surface.

SEM images (Figure 2) of as-deposited and plasma-treated SnO_2 nanowires showed uniform one-dimensional structures with the diameters ranging from 20 to 80 nm. No substantial modification of the nanowire morphology was observed at lower plasma energy (10 W), whereas at higher energies (> 20 W), surface erosion accompanied by enhanced surface roughness was observed (Figure 2c,d) in the samples. High-resolution TEM (HR-TEM) analysis showed a uniform and well-ordered surface structure (Figure 3a) for the untreated TO sample, whereas the influence of plasma treatment and bombardment of energetic ions was evident in TTO4 (Figure 3b), which showed enhanced disorder and depletion of material. The TEM micrograph of TTO4 (inset, Figure 3b) showed 1D heterostructures with a crystalline SnO_2 core and amorphous overlayer and corroborated the assumed structural change by ions possessing higher kinetic energy and impinging on the nanowire surface. The rough amorphous overlayer in plasma-treated samples increases the density of dangling bonds and free lattice sites, thereby favoring surface adsorption phenomena. The existence of an amorphous overlayer was proven by high-resolution TEM (Figure 4b), whereby the FFT of selected overlayers showed the amorphous feature. HR-TEM images of plasma-treated SnO_2 NWs after short (Figure 4a,b) and long (Figure 4c,d) e-beam radiation showed the incipient crystallization and ordering processes on the surface to form crystalline nanoclusters.

Figure 5 shows the X-ray photoelectron spectra of as-deposited and plasma-treated (40 W) SnO_2 nanowires, which showed a distinct shift in the Sn 3d peaks toward a lower binding energy, indicating the chemical reduction of tin species upon exposure to rf plasma. As-deposited SnO_2 sample exhibited the characteristic double peak for the Sn 3d orbital with the main peak (Sn $3d_{5/2}$) at a binding energy of 486.8 eV (FWHM = 1.8), whereas plasma treatment (40 W) caused a narrowing of the Sn $3d_{5/2}$ peak (486.6 eV, FWHM = 1.4), attributed to the conversion of dominated Sn(IV) to mixed Sn(IV)/Sn(II) phases in the surface layers.

Gas-sensing properties of as-deposited and plasma-treated samples of the TTO series showed higher conductance for plasma-treated samples, possibly due to the effect of band bending induced by the surface charges associated with additional states resulting from the shallow donor states of the high number of oxygen vacancies. Figure 6 presents sensitivity (S) against operating temperature (220−250 °C) for as-deposited (TO) and plasma-treated (TTO) SnO_2 nanowire samples. The sensitivity enhancement was found to commensurate with the applied plasma power; for example, the sensitivity of TTO4

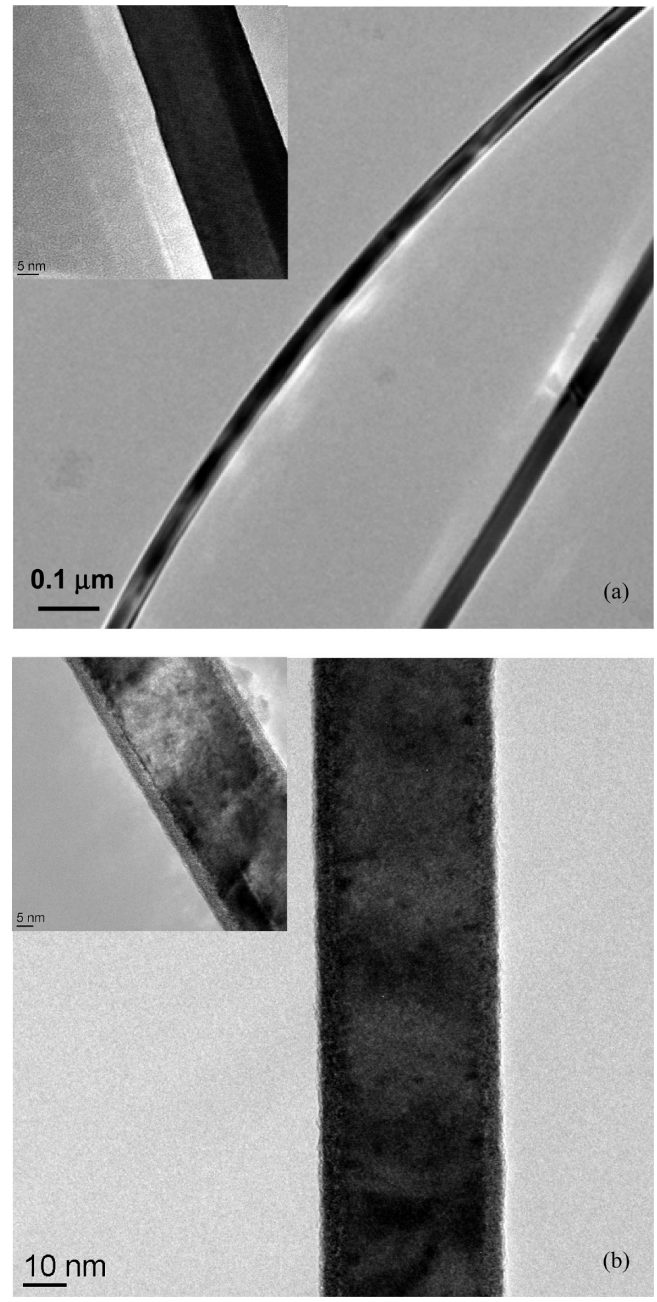

Figure 3. HR-TEM images of (a) as-deposited and (b) plasma-treated (40 W) SnO_2 nanowires.

(4.98) was significantly higher than the value observed for TO (1.69). The sample TTO5 treated with higher plasma power indicated that formation of a significant amount of elemental tin increases the metallic behavior, which is detrimental for the sensitivity of the samples (S = 1.02; 80 W).

Stoichiometric SnO_2 reduced by plasma treatment leads to the creation of bridging oxygen vacancies and less coordinated Sn species (cf. Figure 1), which increases the defect density on the surface. Neutral oxygen adsorbs weakly on the SnO_2 surface with the adsorption energy less than 0.2 eV, whereas on bridging oxygen vacancies, the adsorption energy of up to 1.8 eV was reported.[11] These activated oxygen species passivate the SnO_2 nanowire surface, by withdrawing the electrons from dangling bonds of surface Sn atoms. The bridging oxygen vacancies can bind three O_2 molecules simultaneously with one at the vacancy site and two at 5-fold Sn sites.[29] An increased density of free site and dangling bonds on SnO_2 enhances the amount of

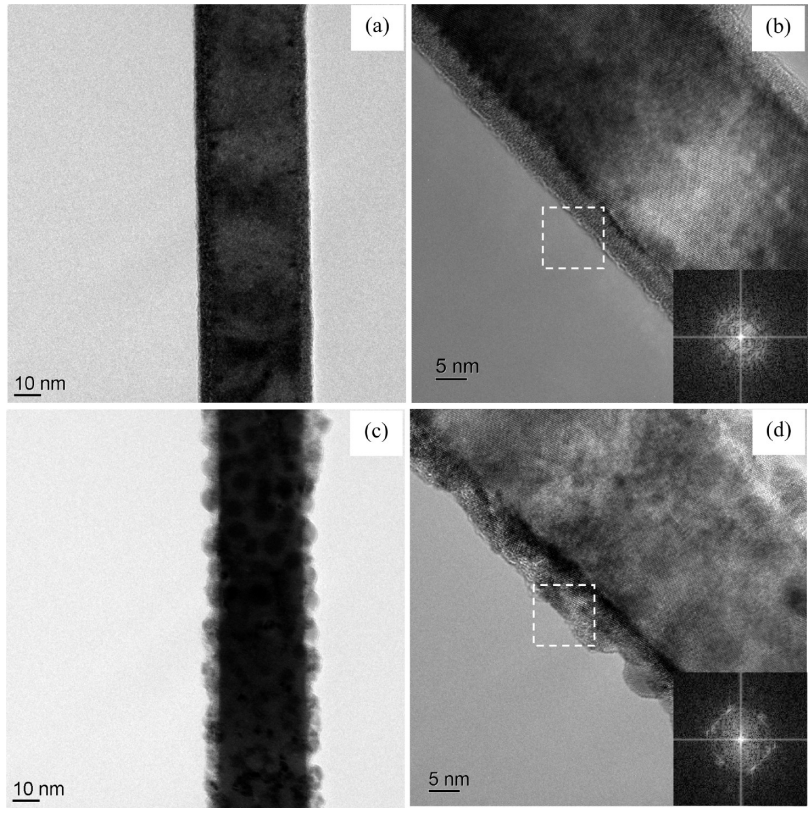

Figure 4. HR-TEM images of plasma-treated SnO_2 NWs after (a, b) short and (c, d) long e-beam radiation showing the e-beam influence on the plasma-treated SnO_2 NWs.

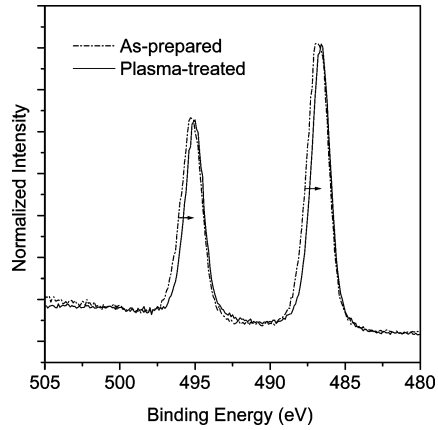

Figure 5. XPS spectra of as-deposited and plasma-treated (40 W) SnO_2 nanowires.

chemisorbed oxygen, as reflected in the higher base resistance of plasma-treated samples. Catalytic oxidation of ethanol on the surface of tin oxide nanowire occurred instantaneously ($CH_3CH_2OH(g) + O_{ads}^- \rightarrow CO + CO_2 + H_2O + e^-$)[30] and was observed as an increase in the conductance of the sample, which was found to be proportional to the applied power in the plasma-treated samples (Figure 6b). This confirmed that the redox reaction at the surface of plasma-treated nanowires with ethanol released more charge carriers into the SnO_2 nanowire conduction band by increasing the cross section of the conducting channels inside the nanowires.[31] It has been recently shown that the charge depletion sheath formed due to the combination of surface defects and underlying bulk structure leads to significant band bending and Fermi level shrinkage in the energy gap.[32] However, the electronic (oxygen vacancies) and structural defects caused by rf plasma treatment modulate the surface electronic structure, hereby shrinking the intrinsic band gap, which leads to enhanced sensing properties. Because plasma treatment resulted in the formation of metallic Sn nanoparticles on the surface of SnO_2 NWs, a decrease in the base resistance (R_{Air}) can be envisaged in the Sn@SnO_2 system. However, the nature of elemental tin leads to a dynamic surface chemistry, resulting in inconsistent gas sensitivity data.

The stability of the plasma-treated (40 W) SnO_2 nanowire gas sensor was checked by on/off gas-sensing measurements. Figure 7 shows that the resistances of as-prepared and plasma-treated SnO_2 NWs (in air and in ethanol) remain relatively unchanged over the entire time period of the experiment. Small drifts were observed within $\pm$ 2% of the resistance, suggesting that the plasma chemically transformed surface of SnO_2 NWs is stable during the gas-sensing process. Experiments to investigate the long-term stability of modified (reduced) SnO_2 NW surfaces are currently underway.

The influence of the surface modification on the intrinsic properties of SnO_2 nanowires was also supported by the photoluminescence (PL) data of as-prepared and plasma-treated SnO_2 nanowires shown in Figure 8. The comparison of the PL of the two samples indicates a red shift (500 $\rightarrow$ 550 nm) due to the possible defect states in the band gap of surface-treated SnO_2 nanowires. The PL intensity (550 nm) of the plasma-treated sample was found to be 4 times higher when compared with the PL signal of the as-prepared sample. The increased PL intensity can be attributed to the increased density of oxygen vacancies (OVs) in the plasma-treated SnO_2 NWs, which is also responsible for the enhanced gas-sensing performance.

It is well-known that the variations in the luminescence of SnO_2 nanowires originate from the surface defect electronic states formed by surface oxygen vacancies. The different types of surface oxygen deficiencies result in the different locations

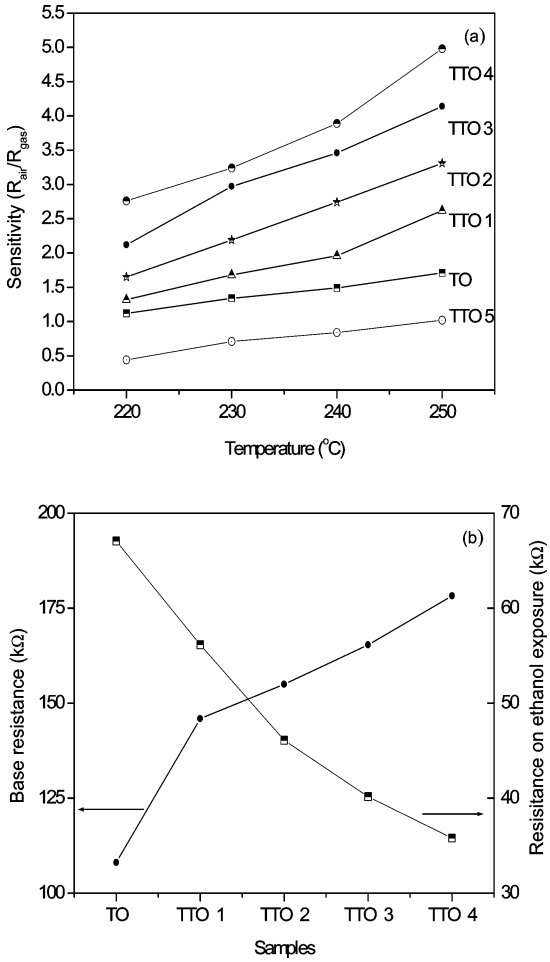

Figure 6. (a) Temperature-dependent sensing response curves for the TTO series samples and (b) base and sensing resistance dependency to the power of plasma treatment, which reveals the increasing oxygen chemisorption over the samples.

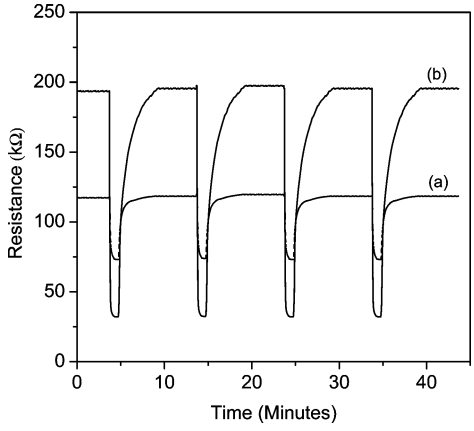

Figure 7. On/off gas-sensing curves of (a) as-prepared and (b) plasma-treated (40 W) SnO_2 nanowires in 100 ppm ethanol at 250 °C.

of defect levels in the forbidden band gap of tin oxide, which are responsible for photoluminescence with different wavelengths. Our experimental results show that the emission peak at 500 nm originates from the surface oxygen vacancies that are created in the CVD process; the peak at 550 nm is due to another type of oxygen vacancy induced by the plasma bombardment. The origin of temperature-dependent photoluminescence in SnO_2 nanowires fabricated by thermal evaporation has been reported (480 and 600 nm) to originate from defect electronic states in the band gap formed by surface oxygen

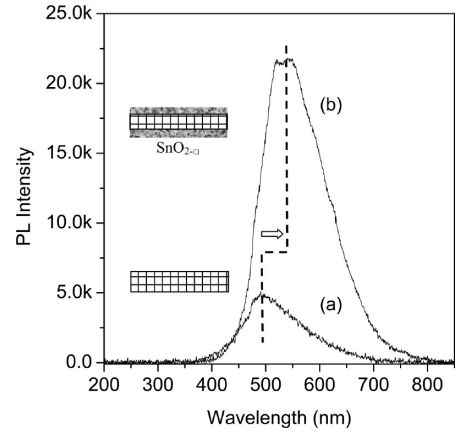

Figure 8. Photoluminescence spectra of as-deposited (TO) and plasma-treated (40 W) SnO_2 nanowires.

vacancies,[33] which supports our observation. As-grown tin oxide nanowires have oxygen vacancies that cause the chemisorption of oxygen on the SnO_2 surface as well as depletion of electrons near the surface. The density of oxygen vacancies is increased in the plasma-treated SnO_2 nanowires due to preferential etching of lattice oxygen atoms, which leads to a higher depletion region and larger surface electric field, resulting in a larger band bending. The sensing experiments carried out with both systems have confirmed the dependence of sensitivity on the density of oxygen vacancies. This plasma effect will be investigated in future experiments with different plasma powers and temperature-dependent and time-resolved photoluminescence.

4. Conclusions

In summary, surface modification of tin oxide nanowires by plasma treatment demonstrates the possibility of engineering the sensing and catalytic properties of metal oxide semiconductors. Plasma treatment on nanoscopic one-dimensional structures allowed modulating the surface (defect) electronic structure and generating intimate amorphous/crystalline oxide interfaces and increased density of oxygen vacancies responsible for efficient charge transfer (transduction) processes, which consequently resulted in enhanced sensitivity. Moreover, the controlled reduction of tin oxide nanowires to the SnO_{2-x}/SnO_2 system opens up new avenues for modifying fundamental properties, such as electronic conductivity, band gap, and electron−hole correlation in reduced dimensionality.

Acknowledgment. Thanks are due to the University of Cologne, German Science Foundation (DFG), Federal Ministry of Education and Research (BMBF), and European Funds (EU-Russia cooperation in FP7 framework) for supporting this work. We are thankful for Ms. I. Grobelsek from Leibniz Institute of New Materials, Saarbrücken, for XRD measurements. Thanks are due to Dr. D. Schaniel, Dr. T. Woike, and Dr. M. Nicoul from University of Cologne for PL measurements.

References and Notes

(1) Cui, Y.; Wei, Q. Q.; Park, H. K.; Lieber, C. M. *Science* **2001**, *293*, 1289.

(2) (a) Kohl, D. *J. Phys. D: Appl. Phys.* **2001**, *34*, R125. (b) Yamazoe, N. *Sens. Actuators, B* **2005**, *108*, 2. (c) Goepel, W.; Hesse, J.; Zemel, J. N. *Sensors: A Comprehensive Survey*; Wiley: New York, 1995. (d) Franke, M. E.; Koplin, T. J.; Simon, U. *Small* **2006**, *2*, 36.

(3) Law, M.; Kind, H.; Messer, B.; Kin, F.; Yang, P. D. *Angew. Chem., Int. Ed.* **2002**, *41*, 2405.

(4) Pan, Z. W.; Dai, Z. R.; Wang, Z. L. *Science* **2001**, *291*, 1947.

(5) (a) Comini, E.; Faglia, G.; Sberverglieri, G.; Pan, Z. W.; Wang, Z. L. *Appl. Phys. Lett.* **2002**, *81*, 1869. (b) Comini, E.; Baratto, C.; Faglia, G.; Ferroni, M.; Vomiero, A.; Sberveglieri, G. *Prog. Mater. Sci.* **2009**, *54*, 1.

(6) Kolmakov, A.; Moskovits, M. *Annu. Rev. Mater. Res.* **2004**, *34*, 151.

(7) (a) Mathur, S.; Barth, S.; Shen, H.; Pyun, J. C.; Werner, U. *Small* **2005**, *1*, 713. (b) Mathur, S.; Ganesan, R.; Grobelsek, I.; Shen, H.; Ruegamer, T.; Barth, S. *Adv. Eng. Mater.* **2007**, *9*, 658.

(8) Hernandez-Ramirez, F.; Tarancon, A.; Casals, O.; Pellicer, E.; Rodriguez, J.; Romano-Rodriguez, A.; Morante, J. R.; Barth, S.; Mathur, S. *Nanotechnology* **2007**, *18*, 424016.

(9) Flippuni, D.; Lundstroem, I. *J. Appl. Phys.* **1988**, *64*, 1274.

(10) Goepel, W.; Schierbaum, K. D. *Sens. Actuators, B* **1995**, *26*, 1.

(11) Batzill, M. *Prog. Surf. Sci.* **2005**, *79*, 47.

(12) Croft, G.; Fuller, M. J. *Nature* **1977**, *269*, 585.

(13) Sakai, G.; Baik, N. S.; Miura, N.; Yamazoe, N. *Sens. Actuators, B* **2001**, *77*, 116.

(14) Zhang, Y.; Kolmakov, A.; Lilach, Y.; Maskovits, M. *J. Phys. Chem. B* **2005**, *109*, 1923.

(15) Hernandez-Ramirez, F.; Tarancon, A.; Casals, O.; Pellicer, E.; Rodriguez, J.; Romano-Rodriguez, A.; Morante, J. R.; Barth, S.; Mathur, S. *Phys. Rev. B* **2007**, *76*, 085429.

(16) Dai, Z. R.; Gole, J. L.; Stout, J. D.; Wang, Z. L. *J. Phys. Chem. B* **2002**, *106*, 1274.

(17) Liu, Z.; Zhang, D.; Han, S.; Li, C.; Tang, T.; Jin, W.; Liu, X.; Lei, B.; Zhou, C. *Adv. Mater.* **2003**, *15*, 1754.

(18) Chen, Y.; Cui, X.; Zhang, K.; Pan, D.; Zhang, S.; Wang, B. *Chem. Phys. Lett.* **2003**, *369*, 16.

(19) Mathur, S.; Shen, H.; Sivakov, V.; Werner, U. *Chem. Mater.* **2004**, *16*, 2449.

(20) Mathur, S.; Shen, H.; Donia, N.; Rugamer, T.; Sivakov, V.; Werner, U. *J. Am. Chem. Soc.* **2007**, *129*, 9746.

(21) Mathur, S.; Barth, S. *Small* **2007**, *3*, 2070.

(22) Sharma, S.; Sunkara, M. K.; Miranda, R.; Lian, G.; Dickey, E. C. *Mater. Res. Soc. Symp. Proc.* **2001**, *676*, Y1.6.1.

(23) Dobrokhotov, V.; Mcllroy, D. N.; Norton, M. G.; Abuzir, A. *J. Appl. Phys.* **2006**, *99*, 104302.

(24) Cabot, A.; Dieguez, A.; Romano-Rodriguez, A.; Morante, J. R.; Barsan, N. *Sens. Actuators, B* **2001**, *79*, 98.

(25) Srivastava, R.; Dwivedi, R.; Srivastava, S. K. *Microelectron. J.* **1998**, *29*, 833.

(26) Chaturvedi, A.; Mishra, V. N.; Dwivedi, R.; Srivastava, S. K. *Microelectron. J.* **2000**, *31*, 283.

(27) Forleo, A.; Francioso, L.; Capone, S.; Casino, F.; Siciliano, P.; Tan, O. K.; Hui, H. *Procedia Chem.* **2009**, *1*, 196.

(28) Hui, H.; Tan, O. K.; Lee, Y. C.; Tran, T. D.; Tse, M. S. *Appl. Phys. Lett.* **2005**, *87*, 163123.

(29) Batzill, M.; Katsiev, K.; Diebold, U. *Appl. Phys. Lett.* **2004**, *85*, 5766.

(30) Idriss, H.; Seebauer, E. G. *J. Mol. Catal. A: Chem.* **2000**, *152*, 201.

(31) Sysoev, V. V.; Goschnick, J.; Schneider, T.; Strelcov, E.; Kolmakov, A. *Nano Lett.* **2007**, *7*, 3182.

(32) Harvey, S. P.; Mason, T. O.; Gassenbauer, Y.; Schafranek, R.; Klein, A. *J. Phys. D: Appl. Phys.* **2006**, *39*, 3959.

(33) Luo, S.; Chu, P. K.; Liu, W.; Zhang, M.; Lin, C. *Appl. Phys. Lett.* **2006**, *88*, 183112.

JP101072F